

Simplified- DP_N treatment of the neutron transport equation

M. Nazari, A. Zolfaghari*, M. Abbasi

Engineering Department, Shahid Beheshti University, Tehran, Iran

Abstract: In this paper the simplified double-spherical harmonics, SDP_N , approximation of the neutron transport equation is proposed. The SDP_N equations are derived from the multi-group DP_N equations for $N = 1, 2, 3$ (comparable to the SP_3 , SP_5 , and SP_7 equations, respectively), and are converted into the form of second order multi-group diffusion equations. The finite element method with the variational approach is then used to numerically solve these equations. The computational performance of the SDP_N method is compared with the SP_N on several fixed-source and criticality test problems. The results show that the SDP_N formulation generally results in parameters like criticality eigenvalue, disadvantage factors, absorption rate, etc. more accurately than the SP_N , even up to an order of magnitude more precise, while the computational effort is the same for both methods.

Keywords: Simplified- DP_N approximation, Simplified- P_N approximation, Neutron transport equation, Finite element method

1. Introduction

The spherical harmonics or P_N equations have been a standard approximation to the neutron transport equation (Davison & Sykes, 1957). The P_N approximation is obtained by expanding the angular dependence of the neutron flux in terms of the spherical harmonic functions and ignoring terms of order $N + 1$ and above. This method gives the exact answer of the transport equation provided that $N \rightarrow \infty$. The P_N equations in the planar one-dimensional geometry are relatively simple and can be cast into the form of $(N + 1)/2$ multi-group diffusion-like equations which are coupled only through the angular moments of the flux. While the number of P_N equations in the planar one-dimensional geometry is limited to only $N + 1$, in three-dimensional case it grows to $(N + 1)^2$ equations. The P_N equations are quite complex in multi-dimensional geometries and cannot be easily formulated in the form of second-order multi-group diffusion equations (Brantley & Larsen, 2000).

The desire for a set of P_N equations in multi-dimensional geometries as simple as those governing in the one-dimensional case caused the introduction of the simplified- P_N (SP_N) equations by Gelbard (1960, 1961). In this approximation, by simply substituting the second-order derivatives for the Laplacian operator, the planar P_N equations are generalized to the multi-dimensional case in an ad-hoc manner. The SP_N method has proven to be a useful approximation to the transport equation in a

* Corresponding author: a-zolfaghari@sbu.ac.ir

variety of situations where diffusion (P_1) theory is inadequate (Lewis & Palmiotti, 1997). For many problems, low order SP_N equations (i.e., SP_3 or SP_5) can capture most of the transport correction to the P_1 approximation (Tomašević & Larsen, 1996). The smaller number of equations—and thus less computational effort—than the multi-dimensional full spherical harmonics approximation, and the possibility of converting the SP_N equations into the multi-group diffusion equations, that can be treated using powerful numerical methods developed for the diffusion theory, are considered as important advantages of the SP_N approximation (Brantley & Larsen, 2000; Lewis & Palmiotti, 1997; Tomašević & Larsen, 1996). Ackroyd et al. (1999) has shown that the full P_N equations, without simplification, could also be formulated as a system of diffusion-like equations. On the downside, the theoretical justification of the SP_N approximation has been controversial but a rigorous resolution of the transport equation into a system of diffusion-like equations was given by Ackroyd et al 1999. A thorough discussion of theoretical aspects of this approximation can be found elsewhere (McClarren, 2011; Sanchez, 2019).

The total neutron flux in the interior of a reactor can be calculated pretty accurately by the P_N approximation (Clark & Hansen, 1964). Because the angular distribution inside a homogeneous medium is almost isotropic, and the spherical harmonics method has an acceptable accuracy in such conditions. However, near points where strong discontinuities in material properties occur, such as vacuum boundaries or regions close to strong absorbers, the angular distribution of flux is usually more anisotropic. These discontinuities cause step changes in the angular flux that their acceptable approximation requires the use of a large number of expansion terms in methods such as the spherical harmonics, which employ full-range angular flux moments. Another problem with the P_N method, and other approximations based on the full-range moments, is the non-convergence of the approximation error near the discontinuities to zero, even though a large N is used (Ziering & Schiff, 1958).

The double-spherical harmonics approximation (DP_N) was proposed by Yvon (1957) to address the problems associated with the P_N method and Ghazaie et al extended to MP_N . The main idea is to use a separate expansion for the neutron angular distribution over each region within which the angular distribution is smoothly and slowly varying, instead of a single expansion for all angles (Clark & Hansen, 1964). In this method, in contrast to the P_N , the half-range angular flux moments are employed instead of the full-range moments to describe the behavior of the angular distribution of neutron more accurately near discontinuities. The important advantage of the DP_N approximation is the exact satisfaction of the vacuum boundary conditions in the planar one-dimensional geometry (Bell & Glasstone, 1970). In problems with severe discontinuities in the neutron angular distribution, the accuracy of the DP_N method is superior to the P_N and is usually comparable to the P_{2N+1} (Stacey,

2007). Recently, Ghazaie et al. (2019) have presented the general MP_N formulation with $M = 1$ and $M = 2$ being the single- and double-spherical harmonics approximations, respectively.

Advantages of the DP_N method over the P_N in the one-dimensional geometry motivated us to put forward the idea of the simplified- DP_N (SDP_N) approximation in this study. Our aim is to introduce the SDP_N method as an alternative to the conventional SP_N approximation, which in addition to neutronics has applications in some other fields (McClarren, 2011). For this purpose in the first stage the odd numbered Legendre moments of coupled set of $2(N+1)$ double- P_N first order differential equations are eliminated to give a system of second-order ordinary equations for the even-numbered Legendre moments. In the next stage, these equations are generalized by replacing the second-order derivatives by Laplacians in the spatial coordinates which are similar to multi-group diffusion equations and the method is called simplified- DP_N . The results will indicate that using the presented SDP_N formulation leads to more accurate values, even up to 10 times more precise, than those obtained using the SP_N method in a given problem. This is despite the fact that for a given $N = 1, 2, \dots$ the mathematical structure of SDP_N and SP_{2N+1} equations and as a result their computational effort is the same. We formulate the SDP_N equations, for $N = 1, 2, 3$, in the second-order form of multi-group diffusion equations, much in the same way as SP_N equations are derived. In this way, the SDP_N method can be easily implemented in an existing code that solves SP_N equations. To solve the SDP_N equations numerically, we employ the Finite Element Method with the variational approach using the Lagrange interpolation functions (Zienkiewicz et al., 2013; Bathe, 2014). The idea of converting the one-dimensional DP_N equations to the form of multi-group diffusion equations dates back to the late 1950s (Anderson et al., 1959; Gelbard et al., 1959). However, no attempt has been made so far—to the authors' knowledge—to investigate the simplified version of the DP_N approximation.

The paper is organized as follows. In section 2, we derive the multi-group SP_N and SDP_N equations from the one-dimensional P_N and DP_N equations, respectively. Numerical treatment of these equations is examined in section 3 making use of the finite element method. In section 4, we compare the numerical results of the proposed SDP_N method with those obtained by the SP_N approximation for several test problems. Conclusions are given in section 5.

2. Derivation of SP_N and SDP_N equations

2.1. Simplified- P_N equations

The steady-state, multi-group P_N equations in one-dimensional geometry have the form (Beckert & Grundmann, 2008)

$$\frac{n+1}{2n+1} \frac{d}{dx} \phi_{n+1,g}(x) + \frac{n}{2n+1} \frac{d}{dx} \phi_{n-1,g}(x) + \Sigma_n^g(x) \phi_{n,g}(x) = Q_{n,g}(x), \quad (1)$$

for $n = 0, 1, \dots, N$ and $g = 1, 2, \dots, G$ where $\phi_{n,g}$ is the n th order flux moment of energy group g and $\Sigma_n^g \equiv \Sigma_t^g - \Sigma_{s,n}^{g \rightarrow g}$. (We have used the standard neutronics notation in the paper.) Assuming an isotropic external source S , the source term in Eq. (1) is given by

$$Q_{n,g}(x) = \sum_{g' \neq g}^G \Sigma_{s,n}^{g' \rightarrow g}(x) \phi_{n,g'}(x) + \delta_{n,0} \left[\frac{\chi_g}{k_{\text{eff}}} \sum_{g'=1}^G \nu \Sigma_f^{g'}(x) \phi_{0,g'}(x) + S_g(x) \right], \quad (2)$$

with $\delta_{n,0}$ being the Kronecker delta. The vacuum boundary condition (Marshak approximation) of Eq. (1) at the left $x = x_b^-$ or right $x = x_b^+$ boundary is expressed as (Stacey, 2007)

$$\sum_{n=0}^N \frac{2n+1}{2} \phi_{n,g}(x_b^\pm) \int_0^{\pm 1} d\mu P_m(\mu) P_n(\mu) = 0, \quad m = 1, 3, \dots, N, \quad (3a)$$

where $P_n(\mu)$ is the Legendre polynomial of order n . The reflective boundary condition requires that

$$\phi_{n,g}(x_b^\pm) = 0, \quad n = 1, 3, \dots, N. \quad (3b)$$

By setting $N = 3$ in Eq. (1), defining $q_g \equiv Q_{0,g}$, and ignoring anisotropic group-to-group scattering (Brantley & Larsen, 2000), i.e.

$$\Sigma_n^{g' \rightarrow g} = 0, \quad n > 0, \quad g' \neq g,$$

we get the four P_3 equations

$$\frac{d}{dx} \phi_{1,g}(x) + \Sigma_0^g(x) \phi_{0,g}(x) = q_g(x), \quad (4a)$$

$$\frac{1}{3} \frac{d}{dx} \phi_{0,g}(x) + \frac{2}{3} \frac{d}{dx} \phi_{2,g}(x) + \Sigma_1^g(x) \phi_{1,g}(x) = 0, \quad (4b)$$

$$\frac{2}{5} \frac{d}{dx} \phi_{1,g}(x) + \frac{3}{5} \frac{d}{dx} \phi_{3,g}(x) + \Sigma_2^g(x) \phi_{2,g}(x) = 0, \quad (4c)$$

$$\frac{3}{7} \frac{d}{dx} \phi_{2,g}(x) + \Sigma_3^g(x) \phi_{3,g}(x) = 0. \quad (4d)$$

These one-dimensional P_3 equations are generalized to the multi-dimensional SP_3 equations following the procedures originally proposed by Gelbard (1960, 1961), i.e. by generalizing the one-dimensional position variable x to the multi-dimensional vector \vec{r} , replacing $\phi_{n,g}$ with $\vec{\phi}_{n,g}$ for odd values of n , and using the divergence and gradient operators instead of the derivatives in x in the even and odd n equations, respectively, in Eqs. (4) we get the SP_3 equations

$$\nabla \cdot \vec{\phi}_{1,g}(\vec{r}) + \Sigma_0^g(\vec{r})\phi_{0,g}(\vec{r}) = q_g(\vec{r}), \quad (5a)$$

$$\frac{1}{3}\nabla\phi_{0,g}(\vec{r}) + \frac{2}{3}\nabla\phi_{2,g}(\vec{r}) + \Sigma_1^g(\vec{r})\vec{\phi}_{1,g}(\vec{r}) = \vec{0}, \quad (5b)$$

$$\frac{2}{5}\nabla \cdot \vec{\phi}_{1,g}(\vec{r}) + \frac{3}{5}\nabla \cdot \vec{\phi}_{3,g}(\vec{r}) + \Sigma_2^g(\vec{r})\phi_{2,g}(\vec{r}) = 0, \quad (5c)$$

$$\frac{3}{7}\nabla\phi_{2,g}(\vec{r}) + \Sigma_3^g(\vec{r})\vec{\phi}_{3,g}(\vec{r}) = \vec{0}, \quad (5d)$$

with the vacuum (\hat{e} is the outward normal)

$$\frac{1}{2}\phi_{0,g}(\vec{r}_b) + \hat{e} \cdot \vec{\phi}_{1,g}(\vec{r}_b) + \frac{5}{8}\phi_{2,g}(\vec{r}_b) = 0, \quad (6a)$$

$$-\frac{1}{8}\phi_{0,g}(\vec{r}_b) + \frac{5}{8}\phi_{2,g}(\vec{r}_b) + \hat{e} \cdot \vec{\phi}_{3,g}(\vec{r}_b) = 0, \quad (6b)$$

and reflective

$$\hat{e} \cdot \vec{\phi}_{n,g}(\vec{r}_b) = 0, \quad n = 1,3, \quad (6c)$$

boundary conditions which are obtained from Eqs. (3). In writing Eqs. (6) it was supposed that the boundary conditions at the right boundary in the one-dimensional geometry apply to all multi-dimensional boundaries (Morel et al., 1996).

We next write Eqs. (5) in the form of a second-order two-group diffusion equation. The second and fourth equation of (5) yield for the odd-order flux moments

$$\vec{\phi}_{1,g}(\vec{r}) = -D_1^g(\vec{r})\nabla\Phi_1^g(\vec{r}), \quad (7a)$$

$$\vec{\phi}_{3,g}(\vec{r}) = -D_2^g(\vec{r})\nabla\Phi_2^g(\vec{r}), \quad (7b)$$

where

$$D_h^g(\vec{r}) \equiv \begin{cases} 1/3\Sigma_1^g(\vec{r}), & h = 1 \\ 1/7\Sigma_3^g(\vec{r}), & h = 2 \end{cases} \quad (8)$$

$$\Phi_h^g(\vec{r}) \equiv \begin{cases} \phi_{0,g}(\vec{r}) + 2\phi_{2,g}(\vec{r}), & h = 1 \\ 3\phi_{2,g}(\vec{r}), & h = 2 \end{cases} \quad (9)$$

Inserting $\vec{\phi}_{1,g}$ and $\vec{\phi}_{3,g}$ from Eqs. (7) in the first and third equation of Eqs. (5), respectively, the four first-order differential equations can be replaced by the following two second-order differential equations (for notational convenience, we will suppress \vec{r} arguments)

$$-\nabla \cdot D_1^g \nabla \Phi_1^g + \Sigma_0^g \Phi_1^g = \frac{2}{3} \Sigma_0^g \Phi_2^g + q_g, \quad (10a)$$

$$-\nabla \cdot D_2^g \nabla \Phi_2^g + \left(\frac{4}{9} \Sigma_0^g + \frac{5}{9} \Sigma_2^g \right) \Phi_2^g = \frac{2}{3} \Sigma_0^g \Phi_1^g - \frac{2}{3} q_g. \quad (10b)$$

The zeroth-order flux moment, i.e. the neutron scalar flux, can be found from Eq. (9):

$$\phi_{0,g} = \Phi_1^g - \frac{2}{3} \Phi_2^g. \quad (11)$$

Substituting odd-order moments given by Eqs. (7) into Eqs. (6), making use of equations (9) and (11), implies the boundary conditions

$$-\hat{e} \cdot \begin{bmatrix} D_1^g \nabla \Phi_1^g \\ D_2^g \nabla \Phi_2^g \end{bmatrix} = \gamma_b \begin{bmatrix} 1/2 & -1/8 \\ -1/8 & 7/24 \end{bmatrix} \begin{bmatrix} \Phi_1^g \\ \Phi_2^g \end{bmatrix}, \quad (12)$$

of the SP_3 equations (10) where $\gamma_b = 1$ and $\gamma_b = 0$ for the vacuum and reflective boundaries, respectively. It should be noted that D_n^g and Φ_n^g are so defined as to guarantee the satisfaction of the interface condition of Eqs. (10) (Anderson et al., 1959). In addition to the SP_3 , we take also into account the SP_5 and SP_7 approximations in this paper. These can be cast into the form of multi-group diffusion equations by proceeding along the same lines as in the derivation of the SP_3 equations. The SP_5 and SP_7 equations along with their boundary conditions are given in the Appendix A (in sections A.1 and A.2, respectively).

2.2. Simplified- DP_N equations

In the double- P_N (DP_N) approximation, the neutron angular flux in the one-dimensional geometry is expanded in terms of the forward (+) and backward (−) half-range flux moments (Bell & Glasstone, 1970)

$$\psi(x, \mu) = \sum_{n=0}^N (2n+1) [\phi_n^-(x) P_n^-(\mu) + \phi_n^+(x) P_n^+(\mu)],$$

with the half-range Legendre polynomials defined as

$$P_n^+(\mu) \equiv \begin{cases} P_n(2\mu - 1), & \mu \geq 0 \\ 0, & \mu < 0 \end{cases},$$

$$P_n^-(\mu) \equiv \begin{cases} 0, & \mu \geq 0 \\ P_n(2\mu + 1), & \mu < 0 \end{cases}.$$

The one-dimensional, steady-state, multi-group DP_N equations read (Stacey, 2007)

$$\begin{aligned} \frac{n}{2n+1} \frac{d}{dx} \phi_{n-1,g}^{\mp}(x) \mp \frac{d}{dx} \phi_{n,g}^{\mp}(x) + \frac{n+1}{2n+1} \frac{d}{dx} \phi_{n+1,g}^{\mp}(x) + 2\Sigma_t^g(x) \phi_{n,g}^{\mp}(x) \\ = Q_{n,g}^{\mp}(x), \end{aligned} \quad (13)$$

for $n = 0, 1, \dots, N$ and $g = 1, 2, \dots, G$ where

$$\begin{aligned} Q_{n,g}^{\mp}(x) = \sum_{g'=1}^G \sum_{m=0}^{2N+1} (2m+1) C_{m,n}^{\mp, \Sigma_{s,m}^{g' \rightarrow g}}(x) \phi_{m,g'}(x) \\ + \delta_{n,0} \left[\frac{\chi_g}{k_{\text{eff}}} \sum_{g'=1}^G \nu \Sigma_f^{g'}(x) \phi_{0,g'}(x) + S_g(x) \right], \end{aligned} \quad (14)$$

is the half-range source term with S being an isotropic external source. The full-range flux moments in Eq. (14) are defined by

$$\phi_{n,g}(x) \equiv \sum_{l=0}^N (2l+1) [C_{n,l}^- \phi_{l,g}^-(x) + C_{n,l}^+ \phi_{l,g}^+(x)],$$

where

$$C_{n,l}^{\pm} \equiv \pm \int_0^{\pm 1} d\mu P_n^{\pm}(\mu) P_l(\mu),$$

are constants. The vacuum and reflective boundary conditions for the DP_N equations (13) are (Lewis & Miller, 1984)

$$\phi_{n,g}^{\pm}(x_b^{\mp}) = 0, \quad n = 0, 1, \dots, N, \quad (15a)$$

and

$$\phi_{n,g}^+(x_b^{\pm}) = (-1)^n \phi_{n,g}^-(x_b^{\pm}), \quad n = 0, 1, \dots, N, \quad (15b)$$

respectively.

By setting $N = 1$ in Eq. (13), after some elementary manipulations, we get the following DP_1 equations (Anderson et al., 1959)

$$\frac{d}{dx} \phi_{1,g}(x) + \Sigma_0^g(x) \phi_{0,g}(x) = q_g(x), \quad (16a)$$

$$\frac{1}{3} \frac{d}{dx} \phi_{0,g}(x) + \frac{2}{3} \frac{d}{dx} \phi_{2,g}(x) + \Sigma_1^g(x) \phi_{1,g}(x) = 0, \quad (16b)$$

$$\frac{3}{8} \frac{d}{dx} \phi_{1,g}(x) + \frac{1}{2} \frac{d}{dx} \phi_{3,g}(x) + \Sigma_2^g(x) \phi_{2,g}(x) = 0, \quad (16c)$$

$$\frac{1}{6} \frac{d}{dx} \phi_{2,g}(x) + \Sigma_3^g(x) \phi_{3,g}(x) = 0, \quad (16d)$$

where

$$q_g(x) = \sum_{g' \neq g}^G \Sigma_{s,0}^{g' \rightarrow g}(x) \phi_{0,g'}(x) + \frac{\chi_g}{k_{\text{eff}}} \sum_{g'=1}^G \nu \Sigma_f^{g'}(x) \phi_{0,g'}(x) + S_g(x),$$

and

$$\Sigma_n^g \equiv \begin{cases} \Sigma_t^g - \Sigma_{s,n}^{g \rightarrow g}, & n = 0,1 \\ \Sigma_t^g - \frac{15}{16} \Sigma_{s,2}^{g \rightarrow g}, & n = 2 \\ \Sigma_t^g - \frac{7}{16} \Sigma_{s,3}^{g \rightarrow g}, & n = 3 \end{cases}.$$

It can be seen that the DP_1 equations (16) are similar to the P_3 equations (4). Following the same procedure that we used in section 2.1 to get the SP_3 equations (5) from the P_3 equations (4), equations of the Simplified- DP_1 (SDP_1) approximation are obtained from Eqs. (16) as

$$\nabla \cdot \vec{\phi}_{1,g}(\vec{r}) + \Sigma_0^g(\vec{r}) \phi_{0,g}(\vec{r}) = q_g(\vec{r}), \quad (17a)$$

$$\frac{1}{3} \nabla \phi_{0,g}(\vec{r}) + \frac{2}{3} \nabla \phi_{2,g}(\vec{r}) + \Sigma_1^g(\vec{r}) \vec{\phi}_{1,g}(\vec{r}) = \vec{0}, \quad (17b)$$

$$\frac{3}{8} \nabla \cdot \vec{\phi}_{1,g}(\vec{r}) + \frac{1}{2} \nabla \cdot \vec{\phi}_{3,g}(\vec{r}) + \Sigma_2^g(\vec{r}) \phi_{2,g}(\vec{r}) = 0, \quad (17c)$$

$$\frac{1}{6} \nabla \phi_{2,g}(\vec{r}) + \Sigma_3^g(\vec{r}) \vec{\phi}_{3,g}(\vec{r}) = \vec{0}, \quad (17d)$$

along with the vacuum

$$\frac{1}{2} \phi_{0,g}(\vec{r}_b) + \hat{e} \cdot \vec{\phi}_{1,g}(\vec{r}_b) + \frac{2}{3} \phi_{2,g}(\vec{r}_b) = 0, \quad (18a)$$

$$-\frac{1}{8} \phi_{0,g}(\vec{r}_b) + \frac{1}{2} \phi_{2,g}(\vec{r}_b) + \hat{e} \cdot \vec{\phi}_{3,g}(\vec{r}_b) = 0, \quad (18b)$$

and reflective

$$\hat{e} \cdot \vec{\phi}_{n,g}(\vec{r}_b) = 0, \quad n = 1,3, \quad (18c)$$

boundary conditions which are concluded from Eqs. (15).

In order to cast equations (17) to the form of multi-group diffusion equations, first the odd-order flux moments are found from the second and fourth equation of (17) as $\vec{\phi}_{1,g} = -D_1^g \nabla \Phi_1^g$ and $\vec{\phi}_{3,g} = -D_2^g \nabla \Phi_2^g$, respectively, with

$$D_h^g(\vec{r}) \equiv \begin{cases} 1/3\Sigma_1^g(\vec{r}), & h = 1 \\ 1/16\Sigma_3^g(\vec{r}), & h = 2' \end{cases} \quad (19)$$

$$\Phi_h^g(\vec{r}) \equiv \begin{cases} \phi_{0,g}(\vec{r}) + 2\phi_{2,g}(\vec{r}), & h = 1 \\ \frac{8}{3}\phi_{2,g}(\vec{r}), & h = 2' \end{cases} \quad (20)$$

By inserting $\vec{\phi}_{1,g}$ and $\vec{\phi}_{3,g}$ in the first and third equation of (17), respectively, we get the second-order SDP_1 equations

$$-\nabla \cdot D_1^g \nabla \Phi_1^g + \Sigma_0^g \Phi_1^g = \frac{3}{4} \Sigma_0^g \Phi_2^g + q_g, \quad (21a)$$

$$-\nabla \cdot D_2^g \nabla \Phi_2^g + \left(\frac{9}{16} \Sigma_0^g + \frac{3}{4} \Sigma_2^g \right) \Phi_2^g = \frac{3}{4} \Sigma_0^g \Phi_1^g - \frac{3}{4} q_g. \quad (21b)$$

Solving for $\phi_{0,g}$ in Eq. (20), the neutron scalar flux could be written as

$$\phi_{0,g} = \Phi_1^g - \frac{3}{4} \Phi_2^g. \quad (22)$$

For the boundary conditions of Eqs. (21) we obtain

$$-\hat{e} \cdot \begin{bmatrix} D_1^g \nabla \Phi_1^g \\ D_2^g \nabla \Phi_2^g \end{bmatrix} = \gamma_b \begin{bmatrix} 1/2 & -1/8 \\ -1/8 & 9/32 \end{bmatrix} \begin{bmatrix} \Phi_1^g \\ \Phi_2^g \end{bmatrix}, \quad (23)$$

from Eqs. (18). Definitions of D_h^g and Φ_n^g are such that the interface condition is satisfied for the SDP_1 equations (Anderson et al., 1959). Derivation of the SDP_2 and SDP_3 approximations (which are equivalent to the SP_5 and SP_7 approximations, respectively) goes in much the same way as that of the SDP_1 . We give equations and boundary conditions for the SDP_2 and SDP_3 cases in the Appendix A (in sections A.3 and A.4, respectively).

3. Solution of the simplified approximation equations using the finite element method

In this section we deal with the numerical treatment of the SP_N and SDP_N equations, which are in the form of multi-group diffusion equations, using the finite element method. To formulate the multi-group diffusion equations variationally in a volume V enclosed with a surface Γ , we employ the functional (Semenza et al., 1972)

$$F_g[\Phi_g] = \frac{1}{2} \int_V dV \left\{ D_g(\vec{r}) [\nabla \Phi_g(\vec{r})]^2 + \Sigma_r^g(\vec{r}) [\Phi_g(\vec{r})]^2 - 2\Phi_g(\vec{r}) S_g(\vec{r}) \right\} + \frac{1}{2} \int_\Gamma d\Gamma \left\{ \gamma_g [\Phi_g(\vec{r})]^2 + 2\Phi_g(\vec{r}) q_g(\vec{r}) \right\}, \quad (24)$$

for $g = 1, 2, \dots, G$ which gives the multi-group diffusion equation

$$-\nabla \cdot D_g(\vec{r})\nabla\Phi_g(\vec{r}) + \Sigma_r^g(\vec{r})\Phi_g(\vec{r}) = S_g(\vec{r}), \quad g = 1, 2, \dots, G, \quad (25)$$

as its Euler-Lagrange equation within V together with the natural boundary condition

$$-\hat{e} \cdot D_g(\vec{r})\nabla\Phi_g(\vec{r}) = \gamma_g\Phi_g(\vec{r}) + q_g(\vec{r}), \quad g = 1, 2, \dots, G,$$

on Γ . The source term in Eq. (24) and (25) has the form

$$S_g(\vec{r}) = \sum_{g'=1}^G \left[(1 - \delta_{g',g})\Sigma_s^{g' \rightarrow g}(\vec{r}) + \frac{1}{k_{\text{eff}}} \chi_g \nu \Sigma_f^{g'}(\vec{r}) \right] \Phi_{g'}(\vec{r}) + s_{\text{ext}}^g(\vec{r}). \quad (26)$$

where s_{ext}^g is the external source in energy group g .

In applying the finite element method, the problem domain $V \cup \Gamma$ is divided into a set of finite elements such that $V = \sum_e V_e$ and $\Gamma = \sum_e \Gamma_e$ with V_e and Γ_e being domain of an element e and its boundary, respectively. The functional of Eq.(24) for an element e takes the form

$$\begin{aligned} F_g^e[\Phi_g] = & \frac{1}{2} D_g^e \int_{V_e} dV (\nabla\Phi_g)^2 + \frac{1}{2} \Sigma_r^{g,e} \int_{V_e} dV (\Phi_g)^2 - \int_{V_e} dV \Phi_g S_g \\ & + \frac{1}{2} \gamma_g^e \int_{\Gamma_e} d\Gamma (\nabla\Phi_g)^2 + \frac{1}{2} \int_{\Gamma_e} d\Gamma \Phi_g q_g. \end{aligned} \quad (27)$$

Summing this equation over all elements leads directly to Eq. (24), which now can be written as

$$F_g[\Phi_g] = \sum_e F_g^e[\Phi_g], \quad (28)$$

where it is assumed that the scalar flux is continuous throughout V .

The scalar flux in an element e is approximated by a piecewise interpolation polynomial

$$\Phi_g(\vec{r}) \approx \Phi_g^e(\vec{r}) = \mathbf{N}_e^T(\vec{r}) \boldsymbol{\Phi}_g^e, \quad \vec{r} \in V_e, \quad (29)$$

where \mathbf{N}_e is the (known) interpolation shape function vector for the element e , and $\boldsymbol{\Phi}^e$ is the vector of the scalar flux (unknown) values associated with nodes of the element. For more detailed discussion of various shape functions and their properties we refer the reader to the literature (Zienkiewicz et al., 2013; Bathe, 2014). Substitution of Eq. (29) into Eq. (27), making use of Eq. (26), yields

$$F_g^e[\boldsymbol{\Phi}_g^e] = \frac{1}{2} (\boldsymbol{\Phi}_g^e)^T \mathbf{A}_g^e \boldsymbol{\Phi}_g^e - (\boldsymbol{\Phi}_g^e)^T \mathbf{f}_g^e, \quad (30)$$

with the matrix \mathbf{A}_g^e defined as

$$\mathbf{A}_g^e = D_g^e \int_{V_e} dV (\nabla \mathbf{N}_e) (\nabla \mathbf{N}_e^T) + \Sigma_r^{g,e} \int_{V_e} dV \mathbf{N}_e \mathbf{N}_e^T + \gamma_g^e \int_{\Gamma_e} d\Gamma \mathbf{N}_e \mathbf{N}_e^T,$$

and

$$\mathbf{f}_g^e = \sum_{g'=1}^G \left[(1 - \delta_{g',g}) \Sigma_{s,g' \rightarrow g}^e + \frac{1}{k_{\text{eff}}} \chi_g \nu \Sigma_{f,g'}^e \right] \left(\int_{V_e} dV \mathbf{N}_e \mathbf{N}_e^T \right) \boldsymbol{\Phi}_{g'}^e + \int_{V_e} dV \mathbf{N}_e S_{\text{ext}}^g - \int_{\Gamma_e} d\Gamma \mathbf{N}_e q_g.$$

Summing Eq. (30) over all elements, according to Eq. (28), gives

$$F_g[\boldsymbol{\Phi}_g] = \frac{1}{2} (\boldsymbol{\Phi}_g)^T \mathbf{A}_g \boldsymbol{\Phi}_g - (\boldsymbol{\Phi}_g)^T \mathbf{f}_g,$$

where $\boldsymbol{\Phi}_g = \sum_e \boldsymbol{\Phi}_g^e$, $\mathbf{A}_g = \sum_e \mathbf{A}_g^e$ and $\mathbf{f}_g = \sum_e \mathbf{f}_g^e$. Finally, minimizing the above equation, i.e. setting its partial derivatives with respect to each of the components of $\boldsymbol{\Phi}_g$ equal to zero, results in the system of linear algebraic equations

$$\mathbf{A}_g \boldsymbol{\Phi}_g = \mathbf{f}_g, \quad g = 1, 2, \dots, G, \quad (31)$$

which can be solved for group scalar fluxes $\boldsymbol{\Phi}_g$. The GMRES method (Saad & Schultz, 1986) without preconditioner and with an error tolerance of 10^{-10} was used to solve the linear system of Eq. (31). Each time after solving Eq. (31), we check whether the group scalar fluxes of the simplified equation, given by Eq. (11) and Eq. (22) for the SP_3 and SDP_1 equations, respectively, are converged using a convergence criterion equal to 10^{-5} . In criticality problems, the largest eigenvalue, i.e. k_{eff} , along with its corresponding eigenvector are calculated with a convergence criterion of 10^{-6} employing the inverse power method (Bathe, 2014).

4. Numerical results

We present our computational results for six test problems. The code to solve the SP_N and SDP_N equations was developed in MATLAB (version 9.4.0). In applying the finite element method, the Lagrangian family of polynomials (Zienkiewicz et al., 2013; Bathe, 2014) were used as interpolation shape functions, and the meshes were generated by the Gmsh (Geuzaine & Remacle, 2009). It should be noted that for all the problems examined here the results of the SP_N and SDP_N approximations are, as expected, clearly superior to those of the P_1 approximation, and we will not discuss this any further in the following.

In the results reported for some of the test cases, it is observed that the accuracy of the value obtained by the SDP_N or SP_N formulation has decreased as the order N has been increased. This is due to the fact that, as discussed in section 1, the SP_N and SDP_N equations are an asymptotic approximation to the transport equation and increasing the order N may not necessarily result in a more precise solution, nor guarantee convergence to the exact solution of the transport equation (Lewis & Palmiotti, 1997; McClarren, 2011). This and some other pertaining issues like what types of problems

the SP_N and SDP_N equations are well suited to, which order N is accurate enough for a given problem, and under what conditions or for which N values the SDP_N method outperforms the SP_N require further research.

4.1. Problem 1: Square source

The first problem is a one-group, fixed-source problem where the system is a square of side length 3.0cm and there is a neutron source of strength $S = 1.0$ in a square of 1.0cm, as shown in Fig. 1. The cross sections of regions 1 and 2 are $\Sigma_t = 1.0\text{cm}^{-1}$, $\Sigma_s = 0.25\text{cm}^{-1}$ and $\Sigma_t = 1.0\text{cm}^{-1}$, $\Sigma_s = 0.5\text{cm}^{-1}$, respectively. A 60×60 mesh of four node bilinear rectangular elements was used to solve this problem. Table 1 lists the absorption rate in region 2 of the system calculated by SP_3 - SP_7 and SDP_1 - SDP_3 methods in comparison to the reference S_{16} results from (Kobayashi et al., 1986). All three SDP_N cases outperform significantly the SP_N cases and SDP_2 has the least error among all. It is notable that the error of the SP_7 case is more than twice that of the SDP_1 . In Fig. 2, the scalar fluxes are plotted along the line $y = 0$ for the SP_3 , SP_5 , SDP_1 and SDP_2 cases together with the reference P_7 result, taken from (Kobayashi et al., 1986). From the beginning to the middle of the x axis, the SDP_1 is more accurate than the SP_3 , whereas the opposite is the case along the other half of the x axis. Overall, the SDP_1 mimics somewhat better than the SP_3 the trend of the reference curve. Regarding the two higher-order approximations in Fig. 2, both the SDP_2 and SP_5 are in good agreement with the reference. Furthermore, Table 1 shows on using SDP_N , one reduces relative error of P_1 result from 16 percent to under 0.2 percent which approves the implemented treatment works very well. The little increase of error from SDP_2 to SDP_3 may be due to extra refinement of variable. In numerical simulation there is an optima level for refinement of variables which beyond it, increasing the number of unknowns and equations causes growing arithmetic operations, round of errors and destroying results.

4.2. Problem 2: Rectangular lattice with circular fuel

This is another one-group, fixed-source problem that contains a circular region, Fig. 3, given in (Wood & Williams, 1973). The cross sections of both regions are $\Sigma_t = 1.0\text{cm}^{-1}$, $\Sigma_s = 0.9\text{cm}^{-1}$ with a uniform source $S = 1.0$ present only in region 2. A mesh composed of three-node linear triangles was used for this problem which is shown in Fig. 3. Thermal disadvantage factors (the ratio of the average scalar flux in region 2 to that of region 1) are compared in Table 2 with reference to the exact value (Wood & Williams, 1973). The SDP_1 and SDP_2 cases are more accurate than their equivalent SP_3 and SP_5 cases, respectively, however the SDP_3 is not as accurate as the SP_7 , which provides the best result for this problem. Errors of the scalar fluxes relative to the exact values at 45 different (x, y) points are

presented in Table 3. Each SDP_N case has less error with respect to its equivalent SP_N case, and the SDP_3 case possesses the least error parameters among all.

4.3. Problem 3: Fuel rods in a square moderator

The one-group, eigenvalue problem in the system shown in Fig. 4 and with the material properties given in Table 4 is considered. We solved this problem using a 100×100 mesh of bilinear rectangular elements. The reference values for this problem are calculated with the S_{16} approximation in (Brantley & Larsen, 2000). Computed values of the criticality eigenvalue k_{eff} are shown in Table 5. All three SDP_N cases calculated more accurate values for k_{eff} than SP_N cases. The best value is for SDP_1 , and both SDP_2 and SDP_3 are more in error relative to the SDP_1 . In Fig. 5, we plot P_1 , SP_3 , SDP_1 , and S_{16} scalar flux distributions along the horizontal lines $y = 4.5\text{cm}$ and $y = 8.967\text{cm}$, respectively. In both cases, fluxes of both the SP_3 and the SDP_1 are much more accurate than the P_1 fluxes and agree pretty well with the S_{16} fluxes.

4.4. Problem 4: Core with hexagonal fuel assemblies

Fig. 6 shows the geometry of this criticality problem which was originally proposed by Hébert (2010) along with a mesh of linear triangular elements used to solve it. One-group, linearly anisotropic cross sections are summarized in Table 6. Table 7 presents the computed values of k_{eff} in which the reference value is obtained by the SP_5 approximation (Hébert, 2010). Since the reference values are computed with the SP_5 approximation, we can only validate the results of the SP_3 and SDP_1 methods for this problem. Although the errors in Table 7 are close, the value calculated by the SDP_1 case is less in error than that of the SP_3 case. Normalized assembly-averaged scalar fluxes of the SP_3 and SDP_1 cases accompanying their error parameters relative to the SP_5 reference values (Dürigen, 2013) are reported in Fig. 7 and Table 8, respectively. Regarding both the maximum and the RMS (Root Mean Square) of relative errors, the SP_3 was not as accurate as the SDP_1 in this problem. This test case showed that the proposed formulation can perform better than the conventional simplified theory in problems with anisotropic scattering.

4.5. Problem 5: BWR cell

This is a two-group, criticality eigenvalue problem from (Stepanek et al., 1982) with geometry and material parameters given in Fig. 8 and Table 9, respectively. A mesh composed of 18×18 bilinear rectangular elements was employed to solve this problem. Table 10 gives the calculated values of k_{eff} together with the disadvantage factors (ratio of the average scalar flux in region 2 to region 1) of the first and second energy groups in comparison to the reference values calculated by SURCU (Stepanek et al., 1982), an integral transport equation code. The most accurate value of k_{eff} belongs to the SDP_3 case, while the SP_7 result is very near to that of the SDP_2 and only slightly better than the one for the

SDP_1 . In respect of disadvantage factors, the SDP_N values for the first group are significantly better than those of the SP_N cases. In the second energy group the SP_N disadvantage factors are more accurate, although the error differences are not as outstanding as in the first group.

4.6. Problem 6: Hexagonal cell with central breeding pin

The last problem from (Hongchun et al., 2007) is a two-group, eigenvalue one for which the geometry is described in Fig. 9. In this figure, the problem's computational mesh made up of linear triangular elements is also shown. Cross sections of regions 1 and 2 are given in Table 9 and region 3 has the same cross sections as region 1. Calculated values of k_{eff} and the ratio of the average scalar flux in regions 2 and 3 to that in region 1 for both energy groups are listed in Table 11 with reference values being obtained by the transmission probability method (Hongchun et al., 2007). Eigenvalues obtained by all three SDP_N cases are more accurate than the SP_7 case, which is the best result of SP_N cases. Considering average scalar flux ratios, in both groups the SDP_N cases outperform SP_N cases in accuracy.

5. Conclusions

The SDP_N approximation was proposed as an improvement to the SP_N method. The second-order multi-group diffusion-like SDP_1 - SDP_3 and SP_3 - SP_7 equations were derived from the multi-group DP_N and P_N equations, respectively. Then, the numerical solution of the equations was discussed employing the finite element method with the variational approach using the Lagrange shape functions. Several fixed-source and criticality eigenvalue test problems were considered to assess the accuracy of the proposed SDP_N approximation compared with the SP_N method.

The results indicated that the SDP_N method outperformed the SP_N in calculating parameters such as the pointwise or assembly-averaged scalar flux distribution, the absorption rate, the criticality eigenvalue, and the group disadvantage factors. The values calculated by the SDP_N equations were in some test cases even up to 10 times more precise than those obtained by the SP_{2N+1} equations for a given order N . In some problems, values calculated by the SDP_1 case were comparable to or even better than those obtained by the SP_7 . In some situations, increasing N in the SDP_N method led to less accurate results, as is the case in the SP_N theory.

Appendix A. Higher order SP_N and SDP_N equations

A.1. SP_5 equations

Multi-group diffusion equation form:

$$-\nabla \cdot D_1^g \nabla \Phi_1^g + \Sigma_0^g \Phi_1^g = \frac{2}{3} \Sigma_0^g \Phi_2^g - \frac{8}{15} \Sigma_0^g \Phi_3^g + q_g,$$

$$-\nabla \cdot D_2^g \nabla \Phi_2^g + \left(\frac{4}{9} \Sigma_0^g + \frac{5}{9} \Sigma_2^g \right) \Phi_2^g = \frac{2}{3} \Sigma_0^g \Phi_1^g + \left(\frac{16}{45} \Sigma_0^g + \frac{4}{9} \Sigma_2^g \right) \Phi_3^g - \frac{2}{3} q_g,$$

$$-\nabla \cdot D_3^g \nabla \Phi_3^g + \left(\frac{64}{225} \Sigma_0^g + \frac{16}{45} \Sigma_2^g + \frac{9}{25} \Sigma_4^g \right) \Phi_3^g = -\frac{8}{15} \Sigma_0^g \Phi_1^g + \left(\frac{16}{45} \Sigma_0^g + \frac{4}{9} \Sigma_2^g \right) \Phi_2^g + \frac{8}{15} q_g.$$

Diffusion coefficients:

$$D_h^g = \begin{cases} 1/3 \Sigma_1^g, & h = 1 \\ 1/7 \Sigma_3^g, & h = 2 \\ 1/11 \Sigma_5^g, & h = 3 \end{cases}$$

Scalar flux:

$$\phi_{0,g} = \Phi_1^g - \frac{2}{3} \Phi_2^g + \frac{8}{15} \Phi_3^g$$

Boundary conditions ($\gamma_b = 1$ and $\gamma_b = 0$ at the vacuum and reflective boundaries, respectively):

$$-\hat{e} \cdot D_h^g \nabla \Phi_h^g = \gamma_b \begin{cases} \frac{1}{2} \Phi_1^g - \frac{1}{8} \Phi_2^g + \frac{1}{16} \Phi_3^g, & h = 1 \\ -\frac{1}{8} \Phi_1^g + \frac{7}{24} \Phi_2^g - \frac{41}{384} \Phi_3^g, & h = 2 \\ \frac{1}{16} \Phi_1^g - \frac{41}{384} \Phi_2^g + \frac{407}{1920} \Phi_3^g, & h = 3 \end{cases}$$

A.2. SP_7 equations

Multi-group diffusion equation form:

$$-\nabla \cdot D_1^g \nabla \Phi_1^g + \Sigma_0^g \Phi_1^g = \frac{2}{3} \Sigma_0^g \Phi_2^g - \frac{8}{15} \Sigma_0^g \Phi_3^g + \frac{16}{35} \Sigma_0^g \Phi_4^g + q_g,$$

$$-\nabla \cdot D_2^g \nabla \Phi_2^g + \left(\frac{4}{9} \Sigma_0^g + \frac{5}{9} \Sigma_2^g \right) \Phi_2^g$$

$$= \frac{2}{3} \Sigma_0^g \Phi_1^g + \left(\frac{16}{45} \Sigma_0^g + \frac{4}{9} \Sigma_2^g \right) \Phi_3^g - \left(\frac{32}{105} \Sigma_0^g + \frac{8}{21} \Sigma_2^g \right) \Phi_4^g - \frac{2}{3} q_g,$$

$$-\nabla \cdot D_3^g \nabla \Phi_3^g + \left(\frac{64}{225} \Sigma_0^g + \frac{16}{45} \Sigma_2^g + \frac{9}{25} \Sigma_4^g \right) \Phi_3^g$$

$$= -\frac{8}{15} \Sigma_0^g \Phi_1^g + \left(\frac{16}{45} \Sigma_0^g + \frac{4}{9} \Sigma_2^g \right) \Phi_2^g + \left(\frac{128}{525} \Sigma_0^g + \frac{32}{105} \Sigma_2^g + \frac{54}{175} \Sigma_4^g \right) \Phi_4^g + \frac{8}{15} q_g,$$

$$-\nabla \cdot D_4^g \nabla \Phi_4^g + \left(\frac{256}{1225} \Sigma_0^g + \frac{64}{245} \Sigma_2^g + \frac{324}{1225} \Sigma_4^g + \frac{13}{49} \Sigma_6^g \right) \Phi_4^g$$

$$= \frac{16}{35} \Sigma_0^g \Phi_1^g - \left(\frac{32}{105} \Sigma_0^g + \frac{8}{21} \Sigma_2^g \right) \Phi_2^g + \left(\frac{128}{525} \Sigma_0^g + \frac{32}{105} \Sigma_2^g + \frac{54}{175} \Sigma_4^g \right) \Phi_3^g - \frac{16}{35} q_g,$$

Diffusion coefficients:

$$D_h^g = \begin{cases} 1/3\Sigma_1^g, & h = 1 \\ 1/7\Sigma_3^g, & h = 2 \\ 1/11\Sigma_5^g, & h = 3 \\ 1/15\Sigma_7^g, & h = 4 \end{cases}$$

Scalar flux:

$$\phi_{0,g} = \Phi_1^g - \frac{2}{3}\Phi_2^g + \frac{8}{15}\Phi_3^g - \frac{16}{35}\Phi_4^g$$

Boundary conditions:

$$-\hat{e} \cdot D_h^g \nabla \Phi_h^g = \gamma_b \begin{cases} \frac{1}{2}\Phi_1^g - \frac{1}{8}\Phi_2^g + \frac{1}{16}\Phi_3^g - \frac{5}{128}\Phi_4^g, & h = 1 \\ -\frac{1}{8}\Phi_1^g + \frac{7}{24}\Phi_2^g - \frac{41}{384}\Phi_3^g + \frac{1}{16}\Phi_4^g, & h = 2 \\ \frac{1}{16}\Phi_1^g - \frac{41}{384}\Phi_2^g + \frac{407}{1920}\Phi_3^g - \frac{233}{2560}\Phi_4^g, & h = 3 \\ -\frac{5}{128}\Phi_1^g + \frac{1}{16}\Phi_2^g - \frac{233}{2560}\Phi_3^g - \frac{3023}{17920}\Phi_4^g, & h = 4 \end{cases}$$

A.3. SDP_2 equations

According to (Anderson et al., 1959), $\Sigma_{s,n}^{g' \rightarrow g}$ must be set equal to zero for $n \geq 3$ and in all energy groups to meet the interface condition of SDP_2 and SDP_3 equations. This does not place any serious limitation on the application of the SDP_2 and SDP_3 approximations, because the simplified approximation is mainly concerned with isotropic scattering problems (McClarren, 2011), and problems with the first or second and higher order of anisotropy are considered beyond the scope of this approximation.

Multi-group diffusion equation form:

$$\begin{aligned} -\nabla \cdot D_1^g \nabla \Phi_1^g + \Sigma_0^g \Phi_1^g &= \frac{5}{144} \Sigma_0^g \Phi_2^g - \frac{17}{144} \Sigma_0^g \Phi_3^g + q_g, \\ -\nabla \cdot D_2^g \nabla \Phi_2^g + \frac{5}{96} \left(\frac{5}{216} \Sigma_0^g + \frac{25}{864} \Sigma_2^g \right) \Phi_2^g &= \frac{5}{144} \Sigma_0^g \Phi_1^g + \frac{5}{96} \left(\frac{17}{216} \Sigma_0^g + \frac{85}{864} \Sigma_2^g \right) \Phi_3^g - \frac{5}{144} q_g, \\ -\nabla \cdot D_3^g \nabla \Phi_3^g + \left(\frac{289}{20736} \Sigma_0^g + \frac{1445}{82944} \Sigma_2^g + \frac{765}{31744} \Sigma_4^g \right) \Phi_3^g &= \\ -\frac{17}{144} \Sigma_0^g \Phi_1^g + \left(\frac{85}{20736} \Sigma_0^g + \frac{425}{82944} \Sigma_2^g - \frac{255}{31744} \Sigma_4^g \right) \Phi_2^g + \frac{17}{144} q_g, \end{aligned}$$

Diffusion coefficients:

$$D_h^g = \begin{cases} \frac{1}{3\Sigma_1^g}, & h = 1 \\ \frac{5}{6144\Sigma_3^g}, & h = 2 \\ \frac{17}{23808\Sigma_5^g}, & h = 3 \end{cases}$$

Scalar flux:

$$\phi_{0,g} = \Phi_1^g - \frac{5}{144}\Phi_2^g + \frac{17}{144}\Phi_3^g$$

Boundary conditions:

$$-\hat{e} \cdot D_h^g \nabla \Phi_h^g = \gamma_b \begin{cases} \frac{1}{2}\Phi_1^g - \frac{1}{96}\Phi_2^g + \frac{1}{96}\Phi_3^g, & h = 1 \\ -\frac{5}{768}\Phi_1^g + \frac{155}{110592}\Phi_2^g - \frac{95}{110592}\Phi_3^g, & h = 2 \\ \frac{17}{1488}\Phi_1^g - \frac{17}{214272}\Phi_2^g + \frac{1343}{214272}\Phi_3^g, & h = 3 \end{cases}$$

A.4. SDP_3 equations

In deriving the following SDP_3 equations we have used some change of variables proposed by (Anderson et al., 1959).

Multi-group diffusion equation form:

$$\begin{aligned} -\nabla \cdot D_1^g \nabla \Phi_1^g + \Sigma_0^g \Phi_1^g &= \frac{2}{3}\Sigma_0^g \Phi_2^g - \frac{145}{5082}\Sigma_0^g \Phi_3^g + \frac{73}{1694}\Sigma_0^g \Phi_4^g + q_g, \\ -\nabla \cdot D_2^g \nabla \Phi_2^g + \left(\frac{4}{9}\Sigma_0^g + \frac{5}{9}\Sigma_2^g\right) \Phi_2^g &= \\ \frac{2}{3}\Sigma_0^g \Phi_1^g + \frac{145}{30492}(4\Sigma_0^g + 5\Sigma_2^g) \Phi_3^g - \frac{73}{10164}(4\Sigma_0^g + 5\Sigma_2^g) \Phi_4^g - \frac{2}{3}q_g, \\ -\nabla \cdot D_3^g \nabla \Phi_3^g + \frac{4205}{1756217232}(340\Sigma_0^g + 425\Sigma_2^g + 432\Sigma_4^g) \Phi_3^g &= \\ -\frac{145}{5082}\Sigma_0^g \Phi_1^g + \frac{145}{30492}(4\Sigma_0^g + 5\Sigma_2^g) \Phi_2^g + \frac{2117}{585405744}(340\Sigma_0^g + 425\Sigma_2^g + 432\Sigma_4^g) \Phi_4^g + \frac{145}{5082}q_g, \\ -\nabla \cdot D_4^g \nabla \Phi_4^g + \frac{1}{168192}\left(292\Sigma_0^g + 365\Sigma_2^g + \frac{91003}{73}\Sigma_4^g\right) \Phi_4^g &= \\ \frac{847}{21024}\Sigma_0^g \Phi_1^g - \frac{847}{126144}(4\Sigma_0^g + 5\Sigma_2^g) \Phi_2^g + \frac{29}{8577792}(340\Sigma_0^g + 425\Sigma_2^g + 432\Sigma_4^g) \Phi_3^g - \frac{847}{21024}q_g, \end{aligned}$$

Diffusion coefficients:

$$D_h^g = \begin{cases} \frac{1}{3\Sigma_1^g}, & h = 1 \\ \frac{1}{7\Sigma_3^g}, & h = 2 \\ \frac{740921}{3317299216\Sigma_5^g}, & h = 3 \\ \frac{881}{15347520\Sigma_7^g}, & h = 4 \end{cases}$$

Scalar flux:

$$\phi_{0,g} = \Phi_1^g - \frac{2}{3}\Phi_2^g + \frac{145}{5082}\Phi_3^g - \frac{73}{1694}\Phi_4^g$$

Vacuum boundary condition (at $\vec{r} = \vec{r}_b$):

$$-\hat{e} \cdot D_h^g \nabla \Phi_h^g = \gamma_b \begin{cases} \frac{1}{2}\Phi_1^g - \frac{1}{8}\Phi_2^g + \frac{417}{125000}\Phi_3^g - \frac{2}{847}\Phi_4^g, & h = 1 \\ -\frac{1}{8}\Phi_1^g + \frac{7}{24}\Phi_2^g - \frac{1137}{200000}\Phi_3^g + \frac{7}{1936}\Phi_4^g, & h = 2 \\ \frac{1}{16}\Phi_1^g - \frac{41}{384}\Phi_2^g + \frac{559}{50000}\Phi_3^g - \frac{235}{54208}\Phi_4^g, & h = 3 \\ -\frac{515}{411136}\Phi_1^g + \frac{103}{51392}\Phi_2^g - \frac{169}{1000000}\Phi_3^g - \frac{215167}{696464384}\Phi_4^g, & h = 4 \end{cases}$$

References

- Ackroyd, R. T., De Oliveira, C. R. E., Zolfaghari, A., Goddard, A. J. H. (1999). On a rigorous resolution of the transport equation into a system of diffusion-like equations. *Progress in Nuclear Energy*, 35(1), 1-64. [https://doi.org/10.1016/S0149-1970\(98\)00024-9](https://doi.org/10.1016/S0149-1970(98)00024-9)
- Anderson, B. L., Davis, J. A., Gelbard, E. M., & Jarvis, P. H. (1959). *FLIP - An IBM-704 Code to Solve the PL and Double-PL Equations in Slab Geometry*.
- Bathe, K. (2014). *Finite Element Procedures* (2nd ed.). Klaus-Jürgen Bathe.
- Beckert, C., & Grundmann, U. (2008). Development and verification of a nodal approach for solving the multigroup SP3 equations. *Annals of Nuclear Energy*, 35(1), 75–86. <https://doi.org/10.1016/j.anucene.2007.05.014>
- Bell, George. I., & Glasstone, S. (1970). *Nuclear Reactor Theory*. Van Nostrand Reinhold Company.
- Brantley, P. S., & Larsen, E. W. (2000). The Simplified P3 Approximation. *Nuclear Science and Engineering*, 134(1), 1–21. <https://doi.org/http://dx.doi.org/10.13182/NSE134-01>
- Clark, M., & Hansen, K. F. (1964). *Numerical Methods of Reactor Analysis* (1st ed.). Academic Press.
- Davison, B., & Sykes, J. B. (1957). *Neutron transport theory*. Oxford University Press.
- Dürigen, S. (2013). *Neutron Transport in Hexagonal Reactor Cores Modeled by Trigonal-Geometry Diffusion and Simplified P3 Nodal Methods*. Karlsruhe Institute of Technology (KIT).

- Ghazaie, S. H., Abbasi, M., Zolfaghari, A. (2019). The Multi-PN approximation to neutron transport equation. *Progress in Nuclear Energy*, 110, 64-74. <https://doi.org/10.1016/j.pnucene.2018.09.001>
- Gelbard, E. M. (1960). *Application of Spherical Harmonics Methods to Reactor Problems*.
- Gelbard, E. M. (1961). *Simplified Spherical Harmonics Equations and Their Use in Shielding Problems*.
- Gelbard, E. M., Davis, J. A., & Pearson, J. (1959). Iterative Solutions to the P1 and Double-P1 Equations. *Nuclear Science and Engineering*, 5, 36–44. <https://doi.org/10.13182/NSE59-A27327>
- Geuzaine, C., & Remacle, J. F. (2009). Gmsh: A 3-D finite element mesh generator with built-in pre- and post-processing facilities. *International Journal for Numerical Methods in Engineering*, 79(11), 1309–1331. <https://doi.org/10.1002/NME.2579>
- Hébert, A. (2010). Mixed-dual implementations of the simplified Pn method. *Annals of Nuclear Energy*, 37(4), 498–511. <https://doi.org/10.1016/J.ANUCENE.2010.01.006>
- Hongchun, W., Pingping, L., Yongqiang, Z., & Liangzhi, C. (2007). Transmission probability method based on triangle meshes for solving unstructured geometry neutron transport problem. *Nuclear Engineering and Design*, 237(1), 28–37. <https://doi.org/10.1016/J.NUCENGDES.2006.04.031>
- Kobayashi, K., Oigawa, H., & Yamagata, H. (1986). The spherical harmonics method for the multigroup transport equation in x-y geometry. *Annals of Nuclear Energy*, 13(12). [https://doi.org/10.1016/0306-4549\(86\)90045-9](https://doi.org/10.1016/0306-4549(86)90045-9)
- Lewis, E. E., & Miller, W. F. (1984). *Computational Methods of Neutron Transport*. John Wiley & Sons.
- Lewis, E. E., & Palmiotti, G. (1997). Simplified Spherical Harmonics in the Variational Nodal Method. *Nuclear Science and Engineering*, 126(1), 48–58. <https://doi.org/10.13182/NSE97-A24456>
- McClarren, R. G. (2011). Theoretical Aspects of the Simplified Pn Equations. *Transport Theory and Statistical Physics*, 39, 73–109. <https://doi.org/10.1080/00411450.2010.535088>
- Morel, J. E., McGhee, J. M., & Larsen, E. W. (1996). A Three-Dimensional Time-Dependent Unstructured Tetrahedral-Mesh SPN Method. *Nuclear Science and Engineering*, 123(3), 319–327. <https://doi.org/10.13182/NSE96-A24196>
- Saad, Y., & Schultz, M. H. (1986). GMRES: A Generalized Minimal Residual Algorithm for Solving Nonsymmetric Linear Systems. *SIAM Journal on Scientific and Statistical Computing*, 7(3), 856–869. <https://doi.org/10.1137/0907058>
- Sanchez, R. (2019). On SPN theory. *Annals of Nuclear Energy*, 129, 331–349. <https://doi.org/https://doi.org/10.1016/j.anucene.2019.01.044>
- Semenza, L. A., Lewis, E. E., & Rossow, E. C. (1972). The Application of the Finite Element Method to the Multigroup Neutron Diffusion Equation. *Nuclear Science and Engineering*, 47, 302–310.
- Stacey, W. M. (2007). *Nuclear Reactor Physics* (2nd ed.). WILEY-VCH.
- Stepanek, J., Auerbach, T., & Hälg, W. (1982). *Calculation of four thermal reactor benchmark problems in XY geometry*.
- Tomašević, D. I., & Larsen, E. W. (1996). The Simplified P2 Approximation. *Nuclear Science and Engineering*, 122(3), 309–325. <https://doi.org/10.13182/NSE96-A24167>

- Wood, J., & Williams, M. M. R. (1973). An integral transport theory calculation of neutron flux distributions in rectangular lattice cells. *Journal of Nuclear Energy*, 27(6).
[https://doi.org/10.1016/0022-3107\(73\)90093-2](https://doi.org/10.1016/0022-3107(73)90093-2)
- Yvon, J. (1957). La diffusion macroscopique des neutrons une methode d'approximation. *Journal of Nuclear Energy (1954)*, 4(3), 305–318. [https://doi.org/10.1016/0891-3919\(57\)90205-X](https://doi.org/10.1016/0891-3919(57)90205-X)
- Zienkiewicz, O. C., Taylor, R. L., & Zhu, J. Z. (2013). *The Finite Element Method: Its Basis and Fundamentals* (7th ed.). Butterworth-Heinemann. <https://doi.org/10.1016/C2009-0-24909-9>
- Ziering, S., & Schiff, D. (1958). Yvon's Method for Slabs. *Nuclear Science and Engineering*, 3(6), 635–647.

Figures

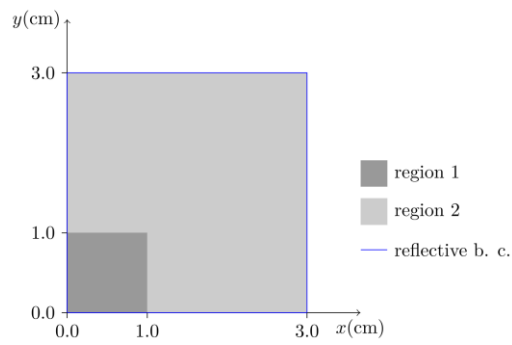


Fig. 1 Geometry of problem 1

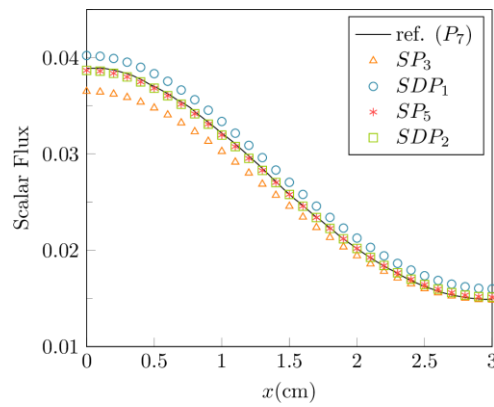


Fig. 2 Scalar flux along the line $y = 0$ for problem 1.

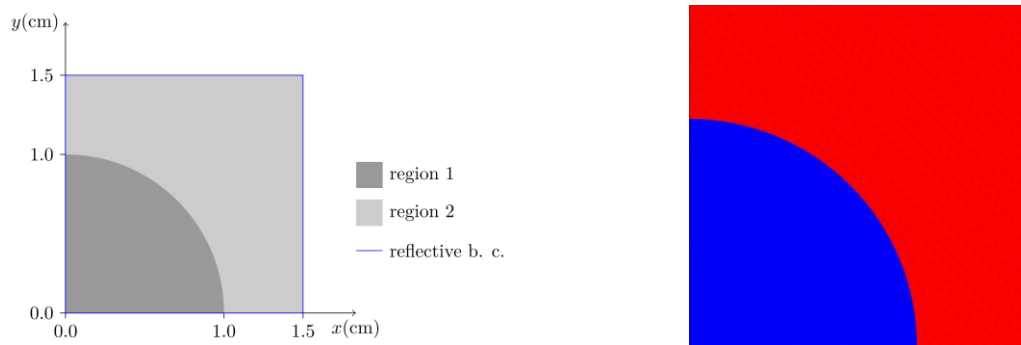


Fig. 3 Geometry (left) and mesh (right) of problem 2

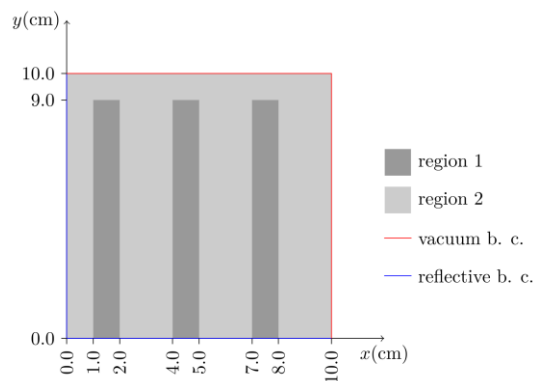


Fig. 4 Geometry of problem 3

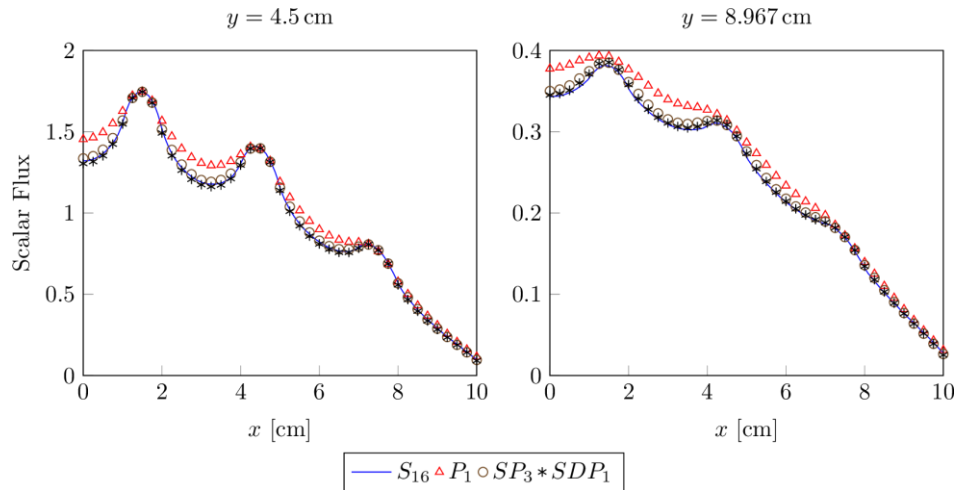


Fig. 5 Scalar fluxes for problem 3

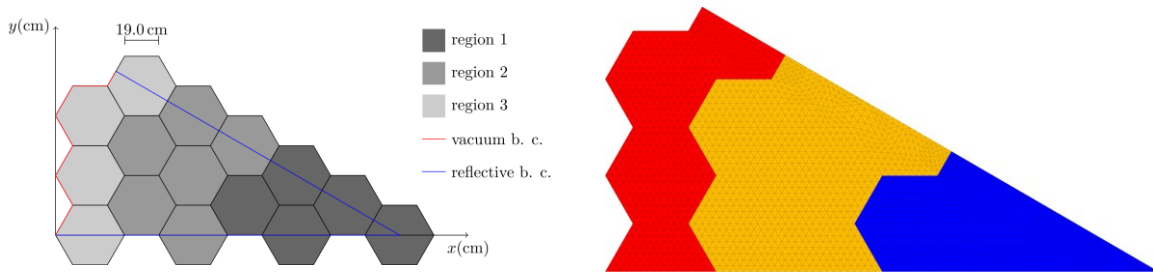


Fig. 6 Geometry (left) and mesh (right) of problem 4

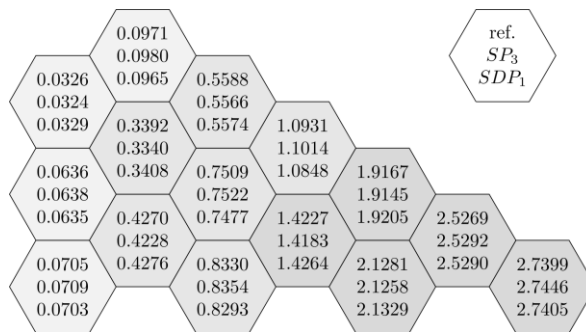


Fig. 7 Normalized assembly-averaged scalar fluxes of problem 4

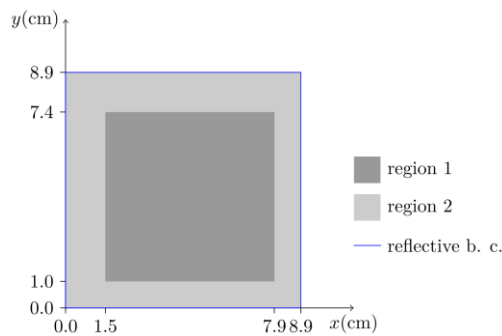


Fig. 8. Geometry of problem 5

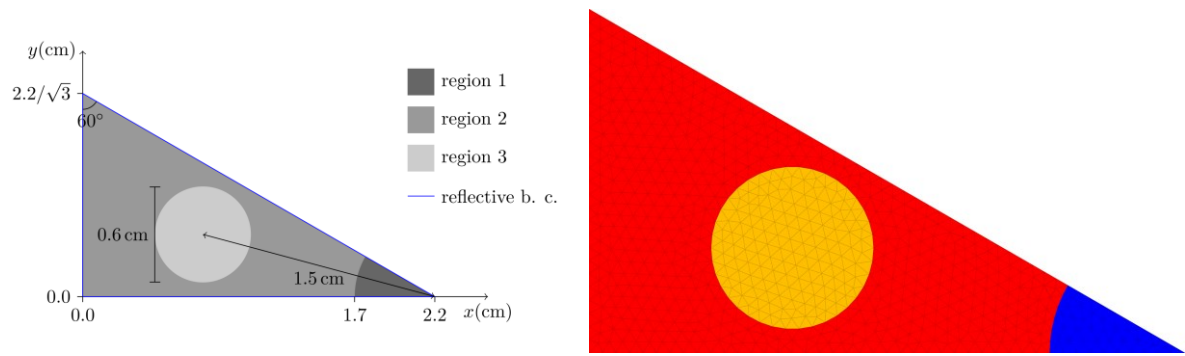


Fig. 9 Geometry (left) and mesh (right) of problem 6

Tables

Table 1 Absorption rates in region 2 of problem 1

	(Ref.)	P_1	SP_3	SP_5	SP_7	SDP_1	SDP_2	SDP_3
Absorption Rate	0.46809	0.39235	0.44931	0.46005	0.46347	0.47037	0.46776	0.46717
Rel. Err. (%)	-	16.1806	4.0120	1.7176	0.9870	-0.4871	0.0705	0.1965
CPU Time (ms)	-	225	256	311	397	257	313	385

Table 2 Disadvantage factors for problem 2

	(Ref.)	P_1	SP_3	SP_5	SP_7	SDP_1	SDP_2	SDP_3
Disadvantage Factor	1.133	1.077	1.119	1.13	1.133	1.141	1.135	1.135
Rel. Err (%)	-	4.943	1.236	0.265	0.000	-0.706	-0.177	-0.177
CPU Time (ms)	-	92	103	115	137	101	114	137

Table 3 Scalar flux error parameters for problem 2

	P_1	SP_3	SP_5	SP_7	SDP_1	SDP_2	SDP_3
RMS of Rel. Errs (%)	2.7952	0.7522	0.3066	0.2122	0.4211	0.1307	0.1032
Max. of Rel. Errs (%)	-5.2448	-1.3536	-0.6689	-0.4886	1.0526	-0.2976	-0.1748

Table 4 Cross sections (cm^{-1}) for problem 3

region	Σ_t	Σ_s	$\nu\Sigma_f$
1	1.50	1.35	0.24
2	1.00	0.93	0.0

Table 5 Criticality eigenvalues for problem 3

	(Ref.)	P_1	SP_3	SP_5	SP_7	SDP_1	SDP_2	SDP_3
k_{eff}	0.806132	0.776518	0.798685	0.802438	0.803168	0.806472	0.803736	0.803479
Rel. Err (%)	-	3.673592	0.923794	0.458238	0.367682	-0.042180	0.297222	0.329102
CPU Time (ms)	-	1328	2408	2894	3522	2418	2864	3543

Table 6 Cross sections (cm^{-1}) for problem 4

region	Σ_t	$\Sigma_{s,0}$	$\Sigma_{s,1}$	$\nu\Sigma_f$
1	0.025	0.013	0.0	0.0155
2	0.025	0.024	0.006	0.0
3	0.075	0.0	0.0	0.0

Table 7 Criticality eigenvalues for problem 4

	(Ref.)	P_1	SP_3	SDP_1
k_{eff}	1.001271	0.97228	1.000186	1.002005

Rel. Err. (%)	-	2.89542	0.108362	-0.073307
CPU Time (ms)	-	204	234	238

Table 8 Error parameters of the normalized assembly-averaged scalar fluxes for problem 4

	P_1	SP_3	SDP_1
RMS of Rel. Errs. (%)	9.3401	0.6312	0.4289
Max. of Rel. Errs. (%)	20.3913	1.5330	0.9202

Table 9 Cross sections (cm^{-1}) for problem 5 and 6

region	g	Σ_t^g	Σ_a^g	$\Sigma_s^{1 \rightarrow g}$	$\Sigma_s^{2 \rightarrow g}$	$\nu \Sigma_f^g$
1	1	1.96647E-1	8.62700E-3	1.78000E-1	1.08900E-3	6.20300E-3
	2	5.96159E-1	6.95700E-2	1.00200E-2	5.25500E-1	1.10100E-1
2	1	2.22064E-1	6.84000E-4	1.99500E-1	1.55800E-3	0.
	2	8.87874E-1	8.01600E-3	2.18800E-1	8.78300E-1	0.

Table 10 Criticality eigenvalues and ratios of the group scalar flux averages for problem 5

	(Ref.)	P_1	SP_3	SP_5	SP_7	SDP_1	SDP_2	SDP_3
k_{eff}	1.2127	1.2210	1.2145	1.2133	1.2130	1.2122	1.2125	1.2126
Rel. Err. (%)	-	-0.6844	-0.1484	-0.0495	-0.0247	0.0412	0.0165	0.0082
$(\bar{\Phi}_2/\bar{\Phi}_1)_1^a$	0.9269	0.9691	0.9473	0.9363	0.9313	0.9267	0.9244	0.9256
Rel. Err. (%)	-	-4.5528	-2.2009	-1.0141	-0.4747	0.0216	0.2697	0.1403
$(\bar{\Phi}_2/\bar{\Phi}_1)_2$	1.2798	1.2285	1.2772	1.2806	1.2809	1.2849	1.2808	1.2815
Rel. Err. (%)	-	4.0084	0.2032	-0.0625	-0.0860	-0.3985	-0.0781	-0.1328
CPU Time (ms)	-	25	38	57	84	37	57	85

^a $(\bar{\Phi}_2/\bar{\Phi}_1)_g$: the ratio of the average scalar flux of group g in region 2 to that in region 1

Table 11 Criticality eigenvalues and ratios of the group scalar flux averages for problem 6

	(Ref.)	P_1	SP_3	SP_5	SP_7	SDP_1	SDP_2	SDP_3
k_{eff}	1.085775	1.090858	1.089170	1.088098	1.087400	1.087152	1.085935	1.085665
Rel. Err. (%)	-	-0.46814	-0.31268	-0.21395	-0.14966	-0.12682	-0.01474	0.010131
$(\bar{\Phi}_2/\bar{\Phi}_1)_1^a$	3.72105	3.78293	3.77609	3.76950	3.76331	3.76373	3.74329	3.72604
Rel. Err. (%)	-	-1.66297	-1.47915	-1.30205	-1.13570	-1.14699	-0.59768	-0.13410
$(\bar{\Phi}_3/\bar{\Phi}_1)_1$	0.23868	0.23492	0.23565	0.23623	0.23666	0.23674	0.23748	0.23749
Rel. Err. (%)	-	1.57533	1.26948	1.02648	0.84632	0.81280	0.50277	0.49858
$(\bar{\Phi}_2/\bar{\Phi}_1)_2$	3.86549	3.81134	3.83055	3.84400	3.85278	3.85577	3.87081	3.87602
Rel. Err. (%)	-	1.40086	0.90390	0.55595	0.32881	0.25146	-0.13763	-0.27241
$(\bar{\Phi}_3/\bar{\Phi}_1)_2$	0.22863	0.23169	0.23050	0.23023	0.23013	0.22995	0.23003	0.23018
Rel. Err. (%)	-	-1.33841	-0.81792	-0.69982	-0.65608	-0.57735	-0.61234	-0.67795
CPU Time (ms)	-	72	108	160	229	106	159	231

^a $(\bar{\Phi}_n/\bar{\Phi}_1)_g$: the ratio of the average scalar flux of group g in region n to that in region 1